frontiers | Frontiers in Earth Science

TYPE Original Research
PUBLISHED 23 August 2022
DOI 10.3389/feart.2022.929538

OPEN ACCESS

EDITED BY
Shu Jiang,
The University of Utah, Salt Lake City, United States

REVIEWED BY
Xiaoping Liu,
China University of Petroleum, Beijing, China
Changan Shan,
Xi'an Shiyou University, Xi'an, China
Shen Zhongmin,
Chengdu University of Technology, Chengdu, China

*CORRESPONDENCE
Tingshan Zhang,
zts_3@126.com

SPECIALTY SECTION
This article was submitted to Geochemistry, a section of the journal Frontiers in Earth Science

RECEIVED 27 April 2022
ACCEPTED 04 July 2022
PUBLISHED 23 August 2022

CITATION
Zeng J, Zhang T, Yang W, Zhu H, Zhang Z, Li H, Bai Y and Gao L (2022), Transitional shale quality and exploration potential: A case study from the Lower Carboniferous Jiusi Formation in northwest Weining, China. *Front. Earth Sci.* 10:929538. doi: 10.3389/feart.2022.929538

Transitional shale quality and exploration potential: A case study from the Lower Carboniferous Jiusi Formation in northwest Weining, China

Jianli Zeng[1], Tingshan Zhang[1]*, Wei Yang[2], Haihua Zhu[1], Zhao Zhang[3], Hongjiao Li[1], Yuhang Bai[1] and Lubiao Gao[1]

[1]School of Geoscience and Technology, Southwest Petroleum University, Chengdu, China, [2]School of Resources and Environmental Engineering, Guizhou Institute of Technology, Guiyang, China, [3]Zhejiang Oilfield Company, Hangzhou, China

The organic-rich shale of the early Carboniferous Jiusi Formation in the Weining area, Southwestern China, has large geological gas reserves, making the Jiusi Formation another target after the Ordovician-Silurian marine shale in South China. The complex superposition of multi-stage tectonic phases since the Himalayan paroxysmal phase has induced a series of controversies in the sedimentology of the Jiui Formation, as only a few drillings were executed. In order to better understand the development potential of the shale associated with the Jiui Formation, five outcrops and a well (YS302) were studied, clarifying the sedimentary evolution of the formation, while two 2D seismic sections were used to analyze the regional structural styles. The result shows that the Jiusi Formation was significantly influenced by the synsedimentary extension of the northwestern margin of the Yadu-Ziyun-Luodian Fault, with the depositional center of the Jiusi Formation extending to well YS302 along a NW direction and asymmetrically thinning in a NE–SW direction. Fifteen lithofacies and three facies associations were identified, from tidal or delta settings to lagoon environments, finally turning into platform facies at the base of the Shangsi Formation. According to the geochemical analysis of 27 core samples and 37 outcrop samples, as well as the well YS302 logging interpretation result. The transitional Jiusi shale in the Weining area has a strong heterogeneity, with high total organic content (TOC) values being mostly provided by the surrounding coal seams. XRD analyses show that the minerals of the transitional shale are dominated by a high clay content (42 wt%). The content of water-sensitive minerals in Jiusi shale is also relatively high, with clay minerals dominated by an illite/smectite mixture (52.8%). When compared with the commercially developed Ordovician-Silurian marine shale, the Jiusi transitional shale shows relatively poor quality, related to dense bioturbation and terrestrial input affecting the preservation of organic matter. Therefore, the evaluation standard for marine shale is difficult to apply to the transitional Jiusi shale. The cumulative thickness of shale in YS302 worthy of shale gas development is nearly 100 m. Meanwhile, considering that the transitional shales are often interlayered with coal, the shale gas and coalbed methane can be developed together.

KEYWORDS

lower Carboniferous, Jiusi transitional shale, shale gas, shale quality, northeastern Weining area

1 Introduction

Starting with 2003, when the United States made a breakthrough in shale gas development, shale gas production began to rise strongly. In 2010, the United States surpassed Russia as the world's largest natural gas producer; until 2016, for the first time, the United States exported more natural gas than it imported. In just 13 years, a global "shale gas revolution" has rapidly reshaped the world's energy landscape (Zou et al., 2017). As an important replacement resource for conventional fossil energy, the potential of shale oil and gas resources has received increasing attention for changing energy structures, ensuring energy security, and promoting technological transformation in the oil and gas industry (Ma et al., 2018). China is one of the earliest countries to evaluate the geological conditions and resource potential of shale gas (Zou et al., 2017). Since 2000, Chinese multi-sectorial cooperation has tracked the theory and technology of shale gas in the United States, as the shale gas industry in China has boomed over the past 20 years. China has already built more than 10^{10} m^3 of natural gas fields in the Sichuan Basin, South China Block (Jiang et al., 2019b), and has become the world's second-largest producer of shale gas (Zou et al., 2017; Ma et al., 2018). Although great progress has been made in shale gas exploration and development in China, the commercial development of shale gas is mainly concentrated in the marine shales of the Ordovician and Silurian Wufeng-Longmaxi Formations in Sichuan Basin and adjacent areas. For developing the shale gas exploration in China, it is necessary to increase the exploration and development of other shales deposits occurring in different areas.

According to the statistics of the Ministry of Natural Resources of China, the geological resources of shale gas occurring at depths shallower than 4500 m are 122 m^3 × 10^{12} m^3, and the recoverable resources are up to 22 m^3 × 10^{12} m^3. The total reserves of shale gas in Guizhou Province reach 10.48 m^3 × 10^{12} m^3 (MNRC, 2018). In Guizhou, the reserves of shale gas confined to the Lower Carboniferous Jiusi Formation were estimated to be 9,595 m^3 × 10^8 m^3, as the depositional center of Jiusi shale occurred in the Weining-Qinglong area (Tang et al., 2014). Yet, most of the Weining area is not yet partitioned for shale gas exploration blocks. Therefore, the comprehensive analysis of the geological conditions of shale gas around Weining has an important guiding role for shale gas exploration and development in the future.

Comprehensive geological surveys in the Weining area began in 1970. At the time, the Geological Team 108 of the Guizhou Geological Bureau proposed the "Weining Trough" concept based on the stratigraphic divisions of the Jiusi Formation and its lithology and thickness (BGMEDGP, 1973). Later, the Weining Trough has been incorporated into the syngenetic extensional fault system bounded by the Yadu-Ziyun-Luodian Fault, which occurs in southern China, crossing the basement and the Palaeozoic–Mesozoic cover. The continuous expansion of this fault system caused the palaeogeographic pattern represented by the alternance of platform and basin conditions since the Devonian and up to the Triassic (Zeng et al., 1995). The Jiusi Formation is one of the main coal-bearing sequences in Guizhou Province. Back in the early days of the geological surveys, the Yadu-Ziyun-Luodian system was considered to not affect the northwest of the Weining area (BGMEDGP, 1973). This situation caused many disputes related to the sedimentary types of the Jiusi Formation in the northwestern Weining area. Starting from 2016, in order to expand the exploration of shale gas, different sedimentary facies analyses were carried out for this shale, showing that the facies of the Jiusi Formation span extremely widely, including the following depositional areas: inner shelf facies (Qin et al., 2016; Tang et al., 2016), fault-controlled lagoon and inner shelf facies (Mei et al., 2021), restricted platform facies (Li, 2016), shore facies to restricted platform facies (Zhang, 2017), shore facies to mixed tidal facies (Sun, 2016), tidal settings (Chen and Zhang, 2020), shore facies to outer shelf facies (Yang, 2020), and transitional settings (Wang et al., 2020). These disputes further hindered the development of the Jiusi shale exploration because the Jiusi shale quality varies greatly in relation to different depositional environments. Therefore the blind deployment of shale gas exploration will cause huge financial losses.

The aim of this paper is to provide geological support for shale gas exploration in the northwestern Weining area (Figure 1). Based on the lithofacies of the Jiusi Formation, our contribution deals with the evolution of facies associations and discusses and resolves the disputes related to sedimentary facies variations. Also, our contribution assesses the quality of the Jiusi shale in relation with key geological parameters, coupled with shale gas evaluation standards, evaluating the Jiusi shale potential.

2 Geological setting

2.1 Tectonics background

Guizhou Province occurs in southwest China, tectonically belonging to the southwest Yangtze Platform, also known as the South China Block (BGMEDGP, 1987). Related to the structural boundary and to the shallow crust deformation in the geological past, the upper Yangtze Block and the Jiangnan orogenic Belt were divided on both sides of the Pan Xian-Guiyang-Tongren fault zone. According to the outcrops thickness and the structure

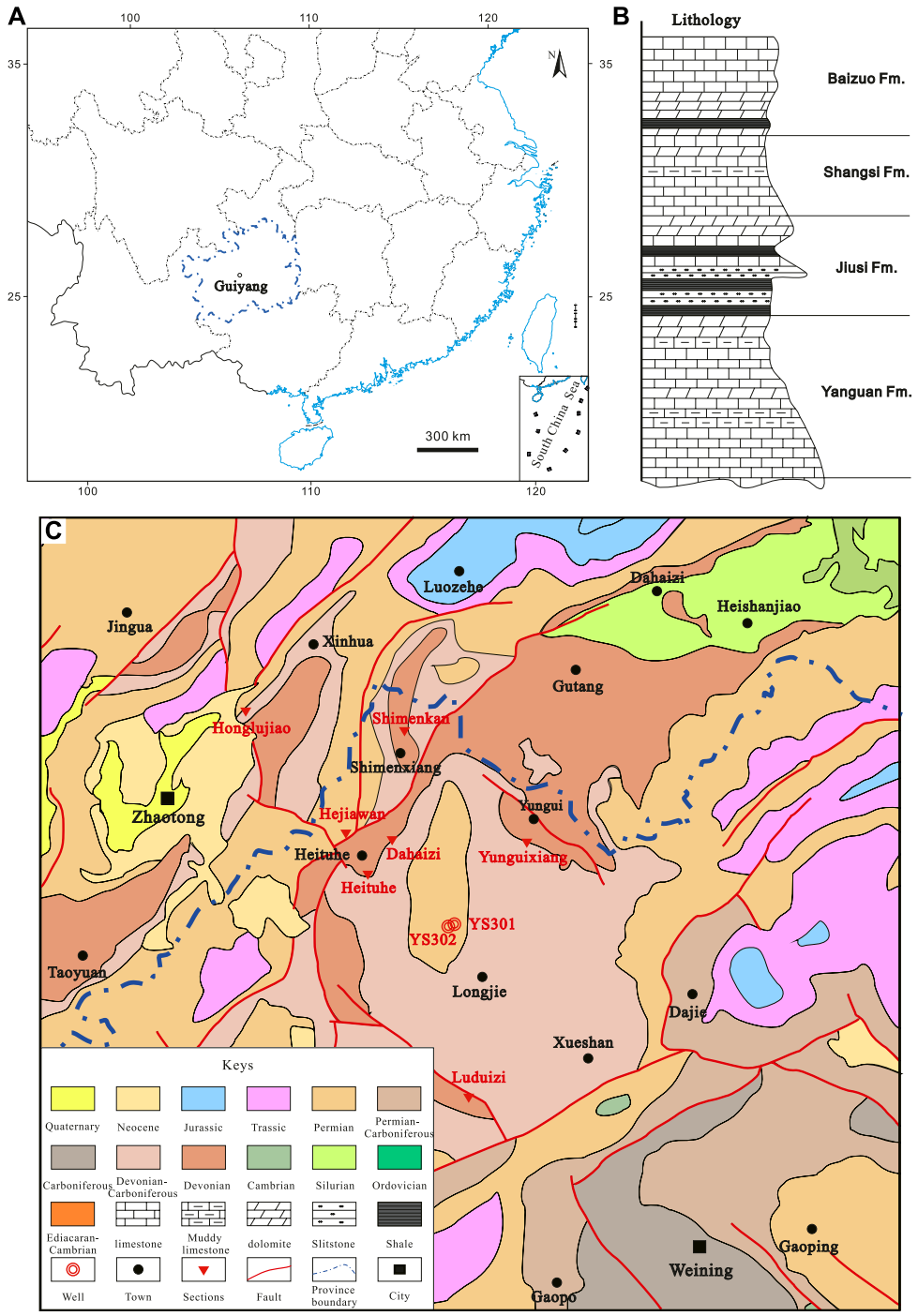

FIGURE 1
Location and general geological structure of the study area. **(A)** Occurrence of Guizhou Province in China. **(B)** The lithology of the Lower Carboniferous in the study area, northeastern Guizhou (modified after Zhang et al., 2017). **(C)** Geological map of the area studied (1:1000000), triangles mark the location of the sections of the Jiusi Formation.

deformation, eight secondary tectonic units were further divided (Figure 2A): Weining Uplift, Liupanshui Depression, northern Guizhou Uplift, Chishui craton Basin, Xingyi Uplift, Youjiang rift-foreland Basin, southern Guizhou Depression, and Rongjiang fold Belt (Figures 2A,B) (BGMEDGP, 1987; BGMEDGP, 2017).

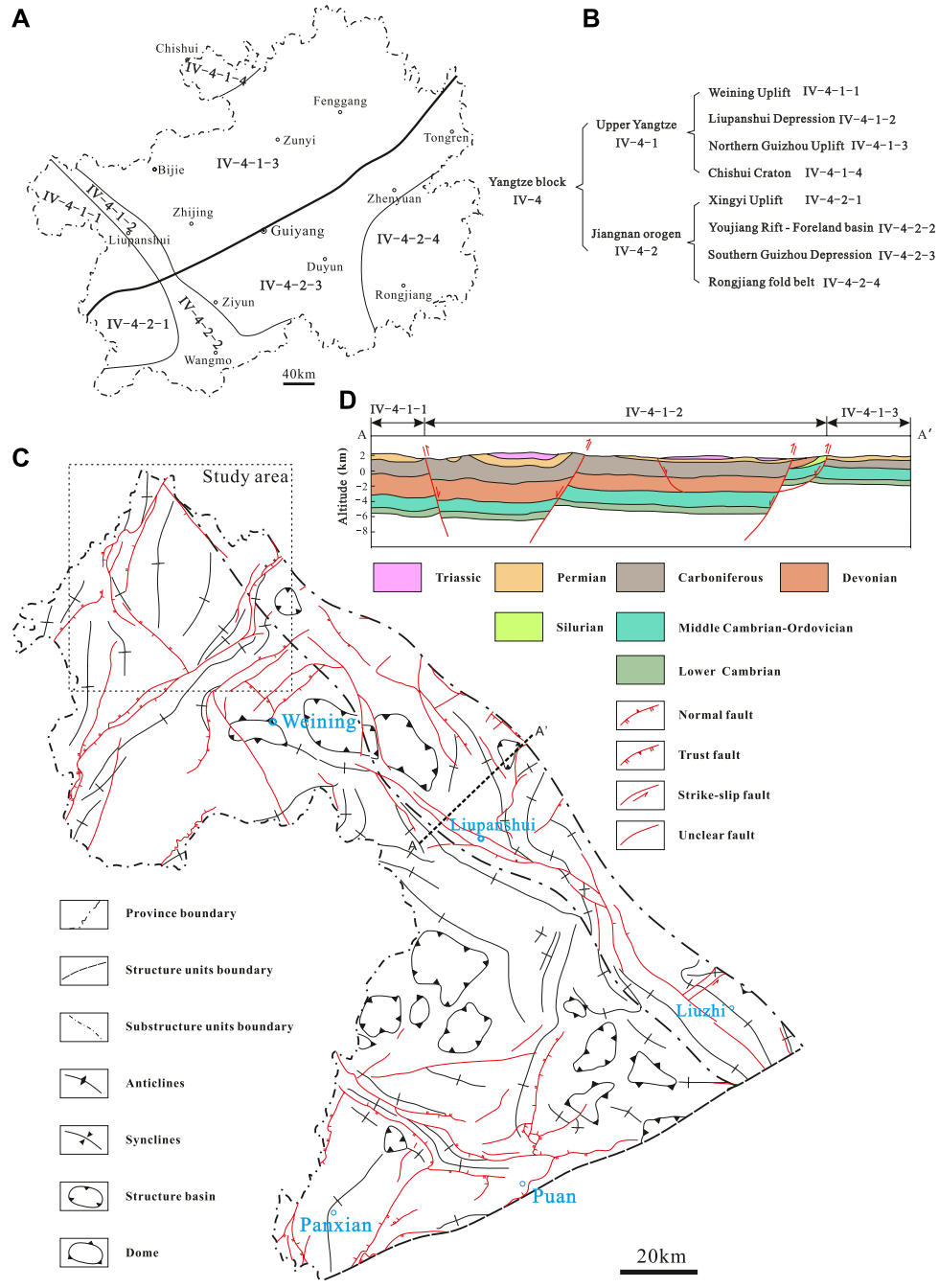

FIGURE 2
Structural outline of the northwestern Guizhou Province. **(A)** The distribution of tectonic units in Guizhou Province. **(B)** Name of each tectonic unit in **A. (C)** The present-day structure outline of the Weining Uplift and of the Liupanshui Depression. **(D)** Geological interpretation of magnetotelluric inversion profiles of continuum media across the Liupanshui Depression (Wang et al., 2013).

The study area covers the Weining Uplift and the Liupanshui Depression (Figure 2C), both structures suffering from complex multi-superpositions of tectonic movements. For instance, in the Weining Uplift, the platform facies developed during the Xueshan-Caledonian cycle, the rift basin facies developed during the Hercynian cycle, and the foreland basin developed during the Indosinian-Yanshan cycle, while the molasse clastic basin was developed during the Himalayan cycle. The present tectonic pattern of the Weining Uplift area is characterized by a dome structure, a gentle brachy-anticline, and a brachy-syncline

arranged alternately along the main linear tectonic directions of the Weining Uplift, oriented NE and NW (Figure 2C) (BGMEDGP, 2017). The Liupanshui Depression is located in the northwest of the Yadu-Ziyun-Luodian fault Zone, an important tectonic boundary in southwest China, associated with various metallic mineral deposits in Guizhou Province (Le, 1991; Xia and Liu, 1992; Cheng and Xu, 1998; Cao et al., 2019; Shi et al., 2019). The present depression includes prolonged and narrow axial NW folds and faults, encompassing Devonian to Jurassic strata involved. Its evolution can be divided into five stages, including the extension crack stage during the early Devonian, the extension-rift stage during the Carboniferous, the strong extension-rift valley stage during the Permian, and the weakened extension-structural inversion stage during the Triassic, and finally, the intracontinental contraction stage after the Yanshan cycle (Wang et al., 2013). As a result of the various extension degrees during different time intervals (Figure 2D), the distribution of deep-water sediments is also variable, controlled by the general SE shrinking (Wang et al., 2006).

2.2 Lithology of Jiusi Formation

The Lower Carboniferous strata are unconformably covered by the Devonian dolomites, with four sets of sequences in ascending order: the Yanguan Formation, the Jiusi Formation, the Shangsi Formation, and the Baizuo Formation (Figure 1B). The Jiusi Formation was originally named the "Chiussu Series" by Ding (1931) in Jiusi village, 12 km west of Pingtang County, Guizhou Province. The Jiusi Formation is unconformably overlaying the Yanguan bioclastic limestone, and it is conformably underlain by the thick, bioclastic limestone Shangsi Formation. In the Weining area, the Jiusi Formation can be divided into two members: the lower member of the Jiusi Formation is mainly clastic, with both marine fauna and terrestrial plants. The lithology of the upper member is represented mainly by dark gray, thick limestone, argillaceous limestone, and black shale, yielding a diverse marine fossil fauna. The overall thickness of the Jiusi Formation ranges between 0 and 992 m (Zhang, 2017).

3 Material and methods

Fieldwork related to the Jiusi Formation was undertaken during the autumn of 2020 when detailed mapping and sampling were carried out from five outcrops and a well (YS302) core section (Discontinuous coring from 1,523.86~1839 m interval, total thickness: 60 m). The five outcrops are: Luduizi (LDZ, N: 27°00′16.4″, E: 104°01′40.9″), Yunguixiang (YGX, N: 27°56′11.97″, E: 104°4′32.66″), Heituhe (HTH, N: 27°14′3203″ E: 103°55′11.25″), Dahaizi (DHZ, N: 27°16′41.48″ E: 103°56′28.37″), and Shimenkan (SMK, N: 27°24′3.65″ E: 103°57′9.8″), respectively (Figure 1C). Five supplementary outcrops and a shallow drill (ZK1402) were considered from published literature and from the Geocloud website* (https://www.geocloud.cgs.gov.cn) for stratigraphic interpretations. The lithology of the Jiusi Formation from different areas is summarized in Table 1. In addition, Zhejiang Oilfield Company provided two 2D seismic sections for stratigraphic correlation.

37 fresh shale/mudstone samples from LDZ and 27 shale samples from the YS302 well were sent to Chengdu University of Technology for analyses related to mineral (including clay) composition, total organic content (TOC). Major elements were analyzed with an X-ray fluorescence spectrometer (XRF-1500), while TOC was tested with a carbon-sulfur analyzer (LECO CS230). Clay mineral analysis was undertaken with an X'Pert Pro diffractometer. All analyses were carried out following the Chinese National Standards GB/T 14506.28-2010 and GB/T 19145-2003. The datasets of major and trace elements, gas content, and porosity results of the whole YS302 well were obtained from Log interpretation, Schlumberger Company.

4 Results

4.1 Lithofacies description and interpretation

We distinguish 15 lithofacies types, summarized in Table 2 with their codes, lithology, descriptions, trace fossils, and body fossil content, together with the interpretation of depositional processes and paleoenvironments.

4.2 Mineralogy

The whole-rock mineral composition of 27 shale samples from YS302 is summarized in Table 3, showing that the shale samples are dominated by clay minerals and quartz, with subordinate calcite and dolomite. The clay mineral content ranges from 14.9% to 71.8% (average 42%). In all samples of the brittle minerals, the quartz content ranges from 10.1% to 80.6% (average 32.1%), the calcite content ranges from 0.7% to 32.5% (average 5.9%), the dolomite content ranges from 1.8% to 29.7% (average 10.7%), and the plagioclase content ranges from 0.6% to 8.1% (average 3.2%), except for the high pyrite content of 37.8% in 1716.41 m. The remaining samples contain less pyrite, and no siderite was detected, except for the samples obtained at the depth of 1833.88 m, accounting for 38.6%.

The clay mineral composition of 26 shale samples from YS302 is also summarized in Table 3, no clay minerals were detected in a shale sample from 1716.41 m. The clay minerals of the YS302 shale are mainly illite/smectite mixed layers, followed

TABLE 1 Lithological dataset of the Jiusi Formation in northeastern Weining.

Sections/Well/ Drill name	Abbreviation	Formation	Sandstone	Mudstone	Carbonatite	Coal	unexposed	Sand ratio/%	Mud ratio/%	Carbonate content/%	Reference
	Thickness/m										
Daihaizi	DHZ	250.4	90.3	150.1	0	0	10	36.1	59.9	0	—
Heituhe	HTH	>207.9	77.3	130.6	0	0	0	37.2	62.8	0	—
Shimenkan	SMK	212.5	73.32	97.3	20.19	7.55	14.14	34.5	45.8	9.5	—
Luduizi	LDZ	327	127	192	6	2	0	38.8	58.7	1.8	—
Yunguixiang	YGX	408.8	45.15	347.1	1.8	0.2	14.55	11	84.9	0.4	—
Dazhangpo	DZP	97.8	35.21	20.59	42	0	0	36	21	42.9	
Xiaofalu	XFL	274	133.5	88.6	51.9	0	0	48.7	32.3	18.9	
Honglujiao	HLJ	68	18.15	49.1	0.75	0	0	26.7	72.2	1.1	
Hejiawan	HJW	378	121.4	252.6	0	4	0	32.1	66.8	0	
Bazhahe	BZH	568	230.58	335.92	0	1.5	0	40.6	59.1	0	BGMEDGP (1987)
YS302	—	835	110	547	171	7	0	13.2	65.5	20.5	—
ZK1402	—	672.4	287.35	234.4	146.81	3.84	0	42.7	34.9	21.8	Geocloud[a]

[a]Geocloud website: http://www.geocloud.cgs.gov.cn.

10.3389/feart.2022.929538

TABLE 2 Lithofacies (LF) of the Jiusi Formation in sections LDZ, YGX, DHZ, and section HTH. BI, bioturbation index (Taylor and Goldring, 1993).

LF	Lithology	Grain size[a]	Description	BI	Biogenic structures	Depositional process and sedimentary environment
M	Mudstones	Silty mud	Dark grey or black grey mudstones, including calcareous mudstone, carbonaceous mudstones, laminated common, with a varying thickness. A few marine fossils	0–1	Macrofossils: few solitary corals, brachiopod, or bryozoan (Figure 6H). Trace fossils: Unidentified	Suspension fallout, low sedimentation rates. Bioclast was transported and deposited during the large tide and storm weather
Mb	Bioturbated Mudstone	Mud-VF	Dark grey or Black grey mudstones. Several meters thick, massive or laminated, locally dense bioturbation. Pyrite was found occasionally	4–6	Trace fossils: *Chondrites, Planolites, Palaeophycus*	Low sedimentation rates. a relative organic-rich, oxygen-deficient tidal zone
Ms	Sigmoidal mudstone	Mud-VF	Dark gray mudstones with thickness from 10 to 30 cm Overall sigmoidal deformation	0	Absent	The soft sediments slide prograde forced by gravity, seaward inclined. The distal delta front environment
Mp	Phytophoric mudstone	Mud-VF	Dark-grey mudstone or carbonaceous mudstones, with abundant plant fossil, sometimes fragmented, varying thickness	0–1	Macrofossils: leaf and trunks of lepidophyte, or unidentified fossils, sometimes fragmented	Low sedimentation rates. Pools of standing water during low-stage channel abandonment; floodplain facies or supratidal environment
C	Coal seam	Mud	Black or black grey coal, generally appear with Mp lithofacies	0–1	Macro fossils: similar with Mp lithofacies	Low sedimentation rates. Typical swamp facies
Ssr	Symmetrical rippled-sandstone	VF-F	White to light grey sandstones with symmetrical ripples. Less than 1–2.5 m	0	Absent	Oscillatory flow above fairweather wave base
Sar	A symmetrical rippled sandstones	VF-F	White to light grey sandstones. Unidirectional current ripples. Current direction: 180°, ripples at the top surface of the sandstones (Figure 7F)	0	Absent	Migration of small ripples in condition of lower flow regime
Sir	Interference rippled sandstone	VF-F	Vari-colored sandstones, ripple acting surface was fuchsia, 15–40 m thick. Contains a few muddy bands (Figure 7G). Quartz content >90%	0	Absent	Fe-cemented surface indicated periods of long exposure. Extremely shallow water environment. Relative high energy. The most proximal ebb-tidal sandy flat
Sc	Cross-bedded sandstones	VF-F-M	White to light grey sandstones. Including awash cross bedding, herringbone bedding and parallel bedding. Thickness varying from 1.5 to 2 m. Erosional, sharp or transitional base	0–1	Trace fossils: unidentified	Continuous reworking and movement of flood and ebb currents. High sedimentation rates. Tidal-dominated environment
Ss	Structureless sandstones	VF-F-M	White to light grey sandstones with a varying thickness. Erosional or sharp base, if sandstones with normal grading. Transitional base if reversing grading	0	Absent	Periodic high-energy discharge with variable flow intensities (bedload and suspended load), Erosion or sharp base indicated a high sedimentation rate
Sb	Bioturbated sandstones	Si-F	Grey to light grey sandstones, transitional base, bioturbated often on the top of the sandstones. Parallel beddings are common. Only 1 bed was exhibited total bioturbated with completely obliterated primary sedimentary structure	4–6	Trace fossils: *Skolithos, Ophiomorpha, Palaeophycus* and unidentified trace fossils	High carrying capacity and bioturbation favorable conditions (optimized oxygen, salinity, temperature)
Hb	Bioturbated heterolithic	Mud-VF	Dark grey–white to light heterolithic, transitional base, beds are serval meters with mud-sand couplets a few centimeters thick. Flaser, lenticular and wavy bedding were common	4–5	Trace fossils: *Skilithos, Ophiomorpha, Palaeophycus, Chondrites, Planolites*	Deposition in alternating energy with local tide influence. From mud-dominated to sand-dominated heterolithics, the energy and water depth get higher and deeper
Lab	Bioturbated arenaceous limestone	—	Grey-light grey arenaceous, trace fossils dominated by *zoophycos* (Fig. 8N, O). Thickness from 0.5 to 1.7 m	2–4	Trace fossils: *Zoophycos*	Sandy particles were probably deposited and transported from the coastal current during the transgressive intermission. Low sedimentation rates. Lagoon environment, with rich food in organic matter for trace maker to build *Zoophycos*
Lc	Chert limestones	—	Black chet (stiff inclusions) embedded in a light grey limestone matrix, chet occurring as lenses. 3.4 m	0	Absent	Pelagic environment (Alvarez et al. (1976); Hein and Karl (1983) or drowned shelf to oceanic seamount settings (Murchey and Jones (1992). Deepwater environment
Lm	Muddy limestones	—	Dark grey- grey muddy limestone, fossils are rare, matrix-supported	0	Absent	Restricted circulation of seawater, low sedimentation rates, lagoon environment

[a]VF, very fine sand; F, fine sand; M, medium sand.

TABLE 3 Mineral compositions of the Jiusi shale samples from YS302.

Depth/m	Mineral constituent content (%)							Relative clay mineral contents (%)					
	Quartz	Plagioclase	Dolomite	Calcite	Pyrite	Siderite	Clay	Smectite	Illite	Kaolinite	Chlorite	I/S	I/S ratio
1,527.54	39.7	2.1	20.2	3.9	4.7	0	29.4	0	15.9	81.1	3	0.3	20
1,527.93	32.9	3.4	10.7	21.5	2.7	0	28.8	0	31	63.2	5	0.7	20
1,528.62	19.4	4.3	29.1	1.1	2.6	0	43.6	0	35.3	61.1	3	0.5	20
1,531.8	22	3.4	29.4	13.1	2.8	0	29.3	0	30.4	62.8	6	1	20
1,532.25	22.8	3.7	29.7	0	1.8	0	42	0	35.6	55	8	1.3	20
1,533.37	29.3	5.5	15.5	4.9	4.2	0	40.6	0	21.3	74.1	4	0.7	20
1,534.19	38	3.9	5.5	2.9	5.6	0	44.1	0	32.1	63.3	4	0.8	20
1,534.58	31.2	5.8	16.9	0.7	4.3	0	41.1	0	26	67.3	6	1.1	20
1,535.94	31.2	4	25.9	0	3.8	0	35.1	0	33.4	61.8	4	0.8	20
1,537.15	30.5	5.2	15.8	8.7	2.2	0	37.5	0	43.4	45.5	11	0	20
1,538.76	41	2.9	12	1.9	2.4	0	39.9	0	22.8	71.4	5	1	20
1,539.47	39.3	4	19.8	0	3.1	0	33.7	0	30	63.8	5	1	20
1,715.65	74.4	0	0	0	10.4	0	15.2	0	23.4	47.1	18	11.7	20
1,716.17	80.6	0	0	0	3.3	0	14.9	0	21.2	53.6	6	19	20
1,716.41	36.8	0	0	0	37.8	0	25.4	—	—	—	—	—	—
1,726.55	15.3	8.1	5.7	32.5	4.1	0	34.3	0	24	60.6	7	8.7	20
1,730.81	19.3	5.9	6.3	23	5	0	40.5	0	28.4	48.1	6	17.3	20
1,813.76	33.4	2.2	4.4	0	1.8	0	58.3	0	18.2	49.4	17	15	20
1,814.32	28.8	4.7	5.5	0	2.1	0	58.8	0	21.2	41.3	18	19.7	20
1,816.8	20.7	3.1	4.8	5.5	2.3	0	63.6	0	22.9	43.8	17	15.9	20
1,817.78	26.5	3	8.1	10.4	1.9	0	50.2	0	24	46.5	15	14.1	20
1,829.27	42.7	2.6	2.3	3.2	1.6	0	47.6	0	20.6	34.5	21	23.5	20
1,830.72	24.4	1.8	0	0	2	0	71.8	0	14.2	26.1	31	28.4	20
1,832.62	21.2	3.7	1.8	0	1.6	0	71.7	0	16.5	36.2	26	21.5	20
1,833.88	10.1	0	4	4.6	0	38.6	39.3	0	12.9	18.1	54	14.5	20
1,834.62	30.1	0.6	8.2	0	1.4	0	59.6	0	27.8	38.6	16	17.8	20
1,837.92	24.7	3.4	6.2	21.6	5.2	0	39	0	21.1	59.5	5	14.2	20

by illite and chlorite. The content of the illite/smectite mixed-layer ranges from 18.1% to 81.1% (average 52.84%), the illite content ranges from 12.9% to 43.4% (average 25.14%), and the chlorite ranged from 0.3% to 28.4% (average 9.63%).

4.3 Total organic content

The TOC content of 27 shale samples from LDZ is summarized in Table 4, with content ranging from 0.5% to 10.4% (average 1.86%). The TOC content of less than 1.0% is accounted for 32.43%, the TOC content ranging from 1.0% to 2.0% is accounted for 35.14%, and the TOC content of more than 2.0% is accounted for 21.62%, 58 shale gas reservoirs of YS302 were evaluated from the logging interpretation of Schlumberger Company. The TOC content of 58 reservoirs ranges from 0.1% to 23.9%, with an average of 3.7%. Notably, TOC content is more than 2%, accounting for 15.52%, and nine reservoirs with TOC content range from 11.6% to 23.9% (average 19.3), all these reservoirs being coal seams. With a TOC content of 0.5% as the lower limit, the TOC content in 35 shale gas reservoirs ranged from 0.6% to 1.7% (average 1.1%).

5 Discussion

5.1 The thickness distribution of the Jiusi Formation around NW weining area

For a long time, the thickness distribution of the Lower Carboniferous Jiusi Formation in Weining and its surrounding areas was elongated along the NW-SE direction of Zhaotong to Liupanshui (GCGB, 2013; Lu

TABLE 4 TOC content result of Jiusi Formation in LDZ.

Samples	TOC (%)	Samples	TOC (%)	Samples	TOC (%)	Samples	TOC (%)	Samples	TOC (%)	Samples	TOC (%)
LDZ-1	0.89	LDZ-7	2.01	LDZ-13	1.28	LDZ-19	0.92	LDZ-25	1.48	LDZ-31	1.01
LDZ-2	1.71	LDZ-8	10.40	LDZ-14	1.06	LDZ-20	0.75	LDZ-26	1.09	LDZ-32	0.50
LDZ-3	0.76	LDZ-9	9.77	LDZ-15	1.60	LDZ-21	0.80	LDZ-27	0.91	LDZ-33	0.70
LDZ-4	1.38	LDZ-10	2.19	LDZ-16	2.44	LDZ-22	0.96	LDZ-28	1.01	LDZ-34	0.89
LDZ-5	1.28	LDZ-11	1.74	LDZ-17	4.03	LDZ-23	1.23	LDZ-29	1.85	LDZ-35	1.03
LDZ-6	3.66	LDZ-12	2.17	LDZ-18	1.47	LDZ-24	0.79	LDZ-30	1.03	LDZ-36	1.09
LDZ-37	0.93										

et al., 2021). The regional depositional center is located at Liudongqiao, on the outskirts of Weining County, with a thickness of 992 m (Zhang, 2017). The thickness distribution of the Jiusi Formation gradually decreases and finally disappears along the NW-SE direction, also rapidly thinning and disappearing to the SW-NE (Tang et al., 2016; Mei et al., 2021). Since, the YS302 well was drilled through the Jiusi Formation showing a thickness of 835 m. This result shows that the previous depositional center may be prolonged along the YS302-Weining line, in a NW-SE direction. Nevertheless, it is still controversial whether the Yadu-Ziyun-Luodian fault extends to the northwest Weining area (YS302), which directly affects the judgment of whether the Jiusi Formation thickness was controlled by the above fault. According to the fault system distribution shown in the geological survey by Geological Team 108, the northwest segment of the Yadu-Ziyun-Luodian fault suspended near Yadu country, and it did not extend to northwestern Weining. But Mao (1997) suggested the fault zone obliquely crosses western Guizhou and extends northwestward to Yunnan Province. Moreover, considering that the study area is less than 5,000 km^2, the thickness of the Jiusi Formation ranges widely, from 0 to 835 m. It was suggested that the northwestern margin of the Liupanshui Depression was still in the process of continuous extension during the early Carboniferous and affected the Weining–Zhaotong area.

The tracking results of the west-east direction seismic event through the YS302 well confirmed this conjecture. The thickness of the Jiusi Formation on the east side of YS302 was controlled by synsedimentary faults, which showed a rapid stage thinning to the east (Figure 3 B-B'). This result is similar to the synsedimentary fault we found outside SMK, with the mudstone layer thickness getting inconsistent on both sides of the fault (Figure 4C). Unfortunately, due to the fact that the seismic section did not cover the west side of the YS302 well, the stratigraphic distribution of the Jiusi Formation along the west side is not clear (Figure 3 B-B'). Tracking results of the seismic event show that the thickness north to south distribution of the Jiusi Formation around the YS302 area is relatively stable, and the stratigraphic thickness in the south of the YS302 decreases rapidly due to the extension of synsedimentary faults, while the thickness of the Jiusi Formation in the north shows a slow thinning trend (Figure 3 C-C').

The synsedimentary extension-fault of the Liupanshui Depression influenced the distribution of the Jiusi Formation, controlled by a graben-horst assemblage (Figure 4B). The datasets from outcrops, from the YS302 well, and from the shallow drill (ZK1402) demonstrate the same scenario. To the northwest of the Weining area, two sedimentary centers in the Jiusi Formation were identified, the main sedimentary center being located in well YS302 and the secondary center being located in ZK1402. To the northeast of YS302, the Jiusi Formation thickness decreases rapidly until the formation disappears. In the southwest area of YS302, the Jiusi Formation thickness first decreases and then increases to ZK1402, further thinning until it disappears (Figure 5).

5.2 Facies associations

5.2.1 Facies association 1 (Lithofacies M, Mb, C, Lab, Lc, Lm): lagoon deposits

Facies association 1 occurs towards the top sections of all five outcrops and in the YS302 well. This sedimentary succession is dominated by laminated calcareous mudstone and carbonaceous mudstone, yielding macrofossils, trace fossils, and pyrite aggregates (Figure 6G), indicating an oxygen-deficient related to an anaerobic lagoonal setting. It begins with the suspension deposits of lithofacies M at YS302 well, DHZ, SMK (Figure 6A), and YGX section (Figure 6B), or lithofacies Lab (bioturbated arenaceous limestone) at LDZ section (Figure 6C), and it ends with the platform facies of the Shangsi Formation. Influenced by sea-level change and by water turbidity, low energy sediments such as lithofacies Mb (Figures 6E,L) and lithofacies C (Figure 6I) were generated during the low systems tract, while lithofacies Lc occurred during the transgressive system tract or maximum flooding surface. Lithofacies Lc (Figure 6K), Lab (Figure 6C), and Lm (Figure 6J) occurred under relatively salt-water

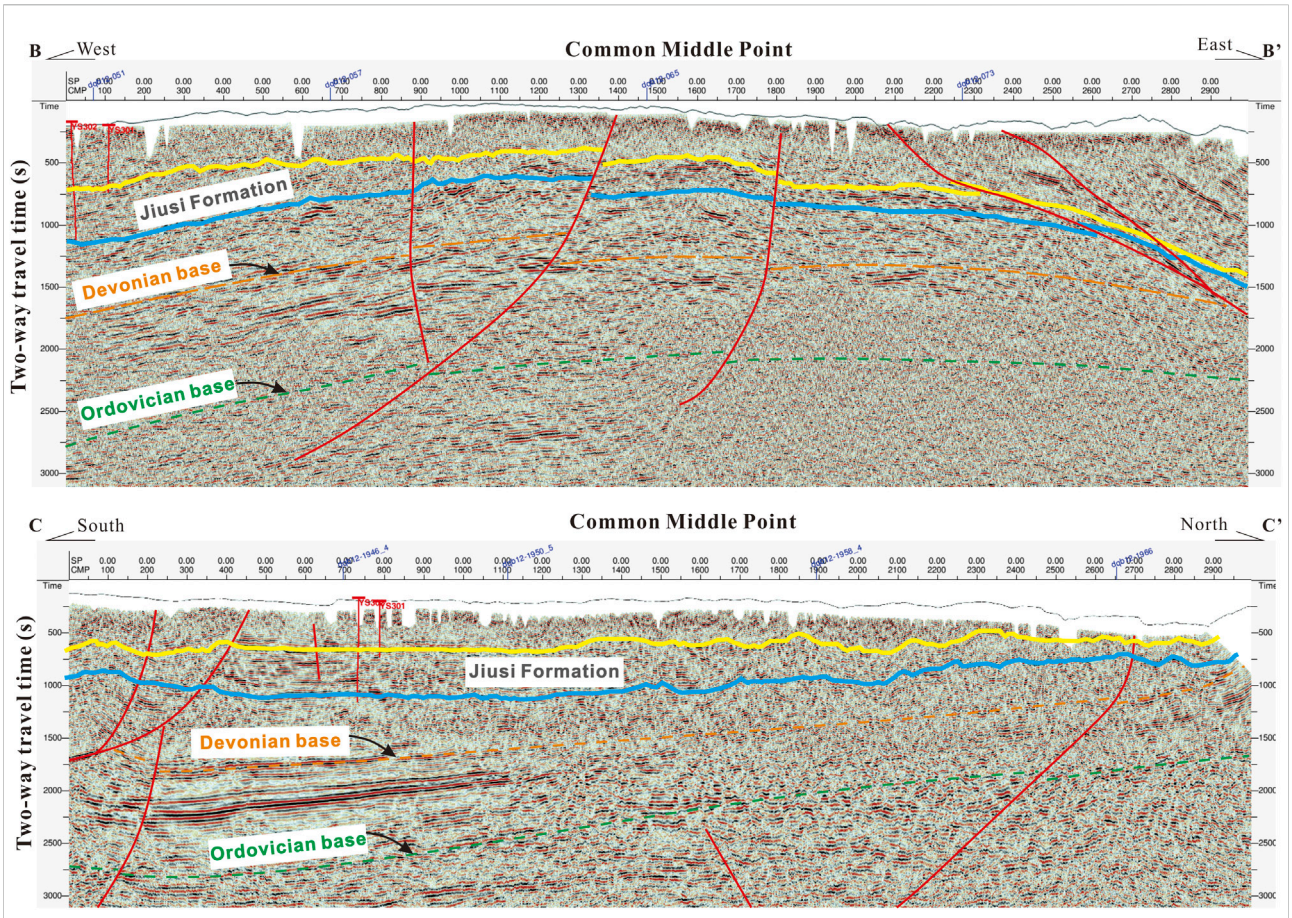

FIGURE 3
Interpreted seismic profiles, including the YS302 well (profile locations shown in Figure 4A). (B-B') West-East direction of the seismic profile cross the YS302 well. (C-C') South-North direction of the seismic profile cross the YS302 well.

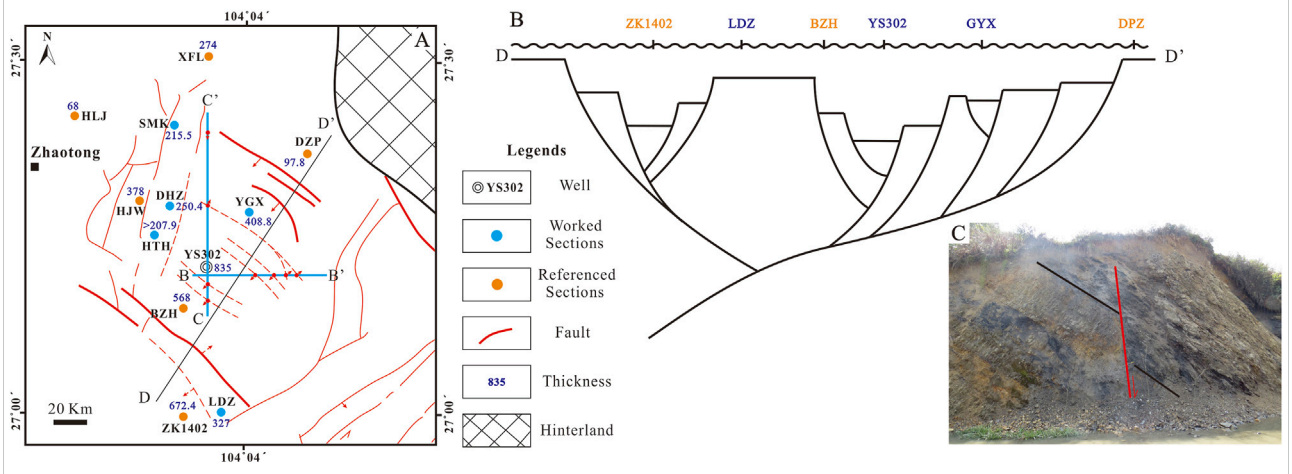

FIGURE 4
The structural pattern in northwestern Weining area. **(A)** The distribution of fault systems and of seismic profile locations in the northwestern Weining area (the fault system distribution was modified after Mao, 1997). **(B)** Synsedimentary extension fault zone in D-D′ section. **(C)** Synsedimentary extension fault within the Jiusi Formation, outside of SMK country.

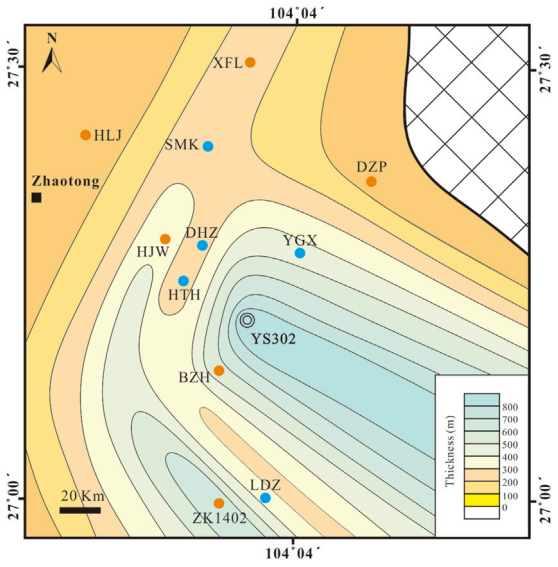

FIGURE 5
Thickness spatial variation of the Jiusi Formation in the northwestern Weining area.

conditions. In the YS302 core section, a few interlaminar, well-preserved solitary corals were the result of subsidence (Figure 6F). Centimetric bioclastic interlayers showed a directional arrangement (Figure 6D) that indicates that the lagoonal setting was disturbed by large storms or tides. In the other four outcrops of the Jiusi Formation, the lagoon deposits are mainly represented by thick (40–80 m), pure mudstones or shales.

Another distinguishing mark of the lagoon facies is represented by the trace fossils and by the geochemical analyses of shales. The trace fossils in the YS302 core section are dominated by *Chondrites* (Figure 6E), although *Chondrites* are an oxygen-deficient to anaerobic paleoxygenation indicator, typically representing the last trace fossil in a bioturbation sequence (Bromley and Ekdale, 1984). However, its appearance ranges from large wild facies, from brackish coastal conditions to deepwater environments (Yang et al., 2004). In the YS302 well, the abundance and size of *Chondrites* increased with the decreasing depth (from 1,540.88 ~ 1,523.86 m), suggesting that the oxygen content increased during the regression cycles. Moreover, the Sr/Ba value, which is a proxy for indicating palaeosalinity (Wang et al., 2020), also showed a wild range in Jiusi shale at YS301 (northeastern 1.2 km to YS302), indicating that the lagoon environment was influenced by a freshwater input.

5.2.2 Facies association 2 (Lithofacies M, Mb, Mp, C, Ssr, Sar, Sir, Sc, Ss, Sb, Hb): tidal deposits

Facies association 2 generally occur in the lower part of the Jiusi Formation in the LDZ, DHZ, SMK, and HTH sections. The composition of sandstones in this association was dominated by well-sorted quartz, with a quartz content usually greater than 90%, marking a tidal environment. The Facies association two begins with tinning- and fining-upward cycles, with an erosive or sharp base, covered by thick middle- or fine-grained structureless sandstones (lithofacies Ss), cross-bedded sandstones (lithofacies Sc) in LDZ (Figures 7C,H), DHZ, and HTH sections, and symmetrical rippled sandstones (Figure 7D) in the SMK section, suggesting a subtidal environment. Passing upwards to very fine sandstone and mudstone (lithofacies M) distributed alternately or to heterolithics, with flaser (Figure 7A), lenticular (Figure 7B), wavy (Figure 7J), and herringbone bedding (Figure 7K), the association indicates a tidal flat environment. Small dunes with erosional bases that disappeared laterally were interpreted as tidal channels and gullies in a sandy flat (Figures 7I,L). These associations end up with lithofacies Mp (phytophoric mudstones) or C (coal) with a large number of leaf fossils, including lepidophytes, and unidentified leaf fossils (Figures 7M,N), representing a supratidal swamp environment. Considering that the supratidal setting is basically an exposed environment and that no exposed marks were found in Mp, the Jiusi Formation recorded rapid transgression conditions, with flood and ebb currents washing away any exposed marks.

The bioturbation was common in this association and it includes the lithofacies Mb (Figure 8G), Sb (Figures 8A–E,H–L), and Hb (Figure 8F). Particularly, the lithofacies Mb in these associations is quite different from the lithofacies Mb in Facies association 1, although tidal bioturbation in lithofacies Mb was also dominated by *Chondrites*. *Chondrites* showed a much higher abundance, diversity, and stronger bioturbation intensity in the tidal environment (Figure 8G), even colonizing adjacent heterolithics (Figure 8F) and sandstones (Figures 8J–L). The bioturbation was profoundly impacted by redox and salinity conditions (Yang et al., 2004). Compared to the oxygen-deficient lagoonal settings, the oxygen-enriched and adequate food supply in the tidal setting, it is more suitable for trace makers to leave their marks. Strong bioturbation is also correlated with sedimentary rates, as the invariable and slow rate of deposition creates a favorable condition for the continuous activity of organisms (Zhang, 2015). Lithofacies Sb at the lower part of LDZ in this association even involved a total bio-disturbed sandstone (Figures 8J–L).

Different kinds of ichnotaxa are widely found in these associations, including *Skolithos* (Figures 8A–C), *Ophiomorpha* (Figures 8D,E), *Palaeophycus* (Figures 8H,I), *Chondrites*, and *Planolites* (Figure 8M). In the lithofacies Sb, the trace fossils *Skolithos* and *Ophiomorpha* belong to the *Skoithos* ichnofacies, which typically occur in lower intertidal to shallow subtidal environments with moderately to well-sorted, shifting sandy substrates related to sedimentation and erosion rates (Yang et al., 2004; MacEachern et al., 2012). As discussed above (see section 5.2.1), the occurrence of *Chondrites*, together with

FIGURE 6
Facies association 1. **(A)** Lithofacies M, section SMK. **(B)** Lithofacies M, section YGX. **(C)** Lithofacies Lab (bioturbated arenaceous limestone) with abundant *Zoophycos*, section LDZ. **(D)** Lithofacies M, calcareous shale, bioclast interlayer showed directional arrangement (yellow arrow), 1,525.51–1525.61 m, YS302. **(E)** Lithofacies Mb (bioturbated mudstone) with abundant chondrites (yellow arrow). 1,526.30–1526.48 m, YS302. **(F)** Lithofacies M with solitary corals (yellow arrow) 1729.56–1729.68 m YS302. **(G)** Pyrite aggregate (yellow arrow) in lithofacies M, 1817.70–1817.88 m, YS302. **(H)** Bryozoan fossils (yellow arrow) in lithofacies M, 1830.10–1830.27 m, YS302. **(I)** Lithofacies C (coal), 1839.55–1839.75 m, YS302. **(J)** Lithofacies Lm (muddy limestone), calcareous bond interlayer within muddy limestone (yellow arrow), 1,527.02–1527.22 m, YS302. **(K)** Lithofacies Lc (chet limestone), section YGX. **(L)** Lithofacies Mb, Chondrites (yellow arrow), section DHZ.

FIGURE 7
Facies association 2, intertidal or subtidal zone. **(A)** Heterolithic with flaser bedding, section SMK. **(B)** Heterolithic with lenticular bedding, section DHZ. **(C)** Lithofacies Sc (cross-bedded sandstones) with awash cross-bedding, section LDZ. **(D)** Lithofacies Ssr (Symmetrical rippled sandstones), section SMK. **(E)** Lithofacies Sir (interference rippled sandstones), section SMK. **(F)** Lithofacies Sar (asymmetrical rippled sandstones) with the current direction of 180°, section HTH. **(G)** Quartz sandstone with muddy bands, section SMK. **(H)** Lithofacies Sc with awash cross-bedding, section LDZ. **(I)** Small dunes with erosional base, disappearing laterally (yellow dashed line), gully setting, section LDZ. **(J)** Lithofacies Sc with wavy cross-bedding, section DHZ. **(K)** Lithofacies Sc with parallel bedding and herringbone bedding (yellow arrow), section DHZ. **(L)** Repeated seven finning upwards cycles with erosional bases of each sequence, tidal channel setting, section HTH. (continued). Facies association 2, supratidal zone. Lithofacies Mp with abundant unidentified leaf fossil, section LDZ **(M)** and section SMK **(N)**.

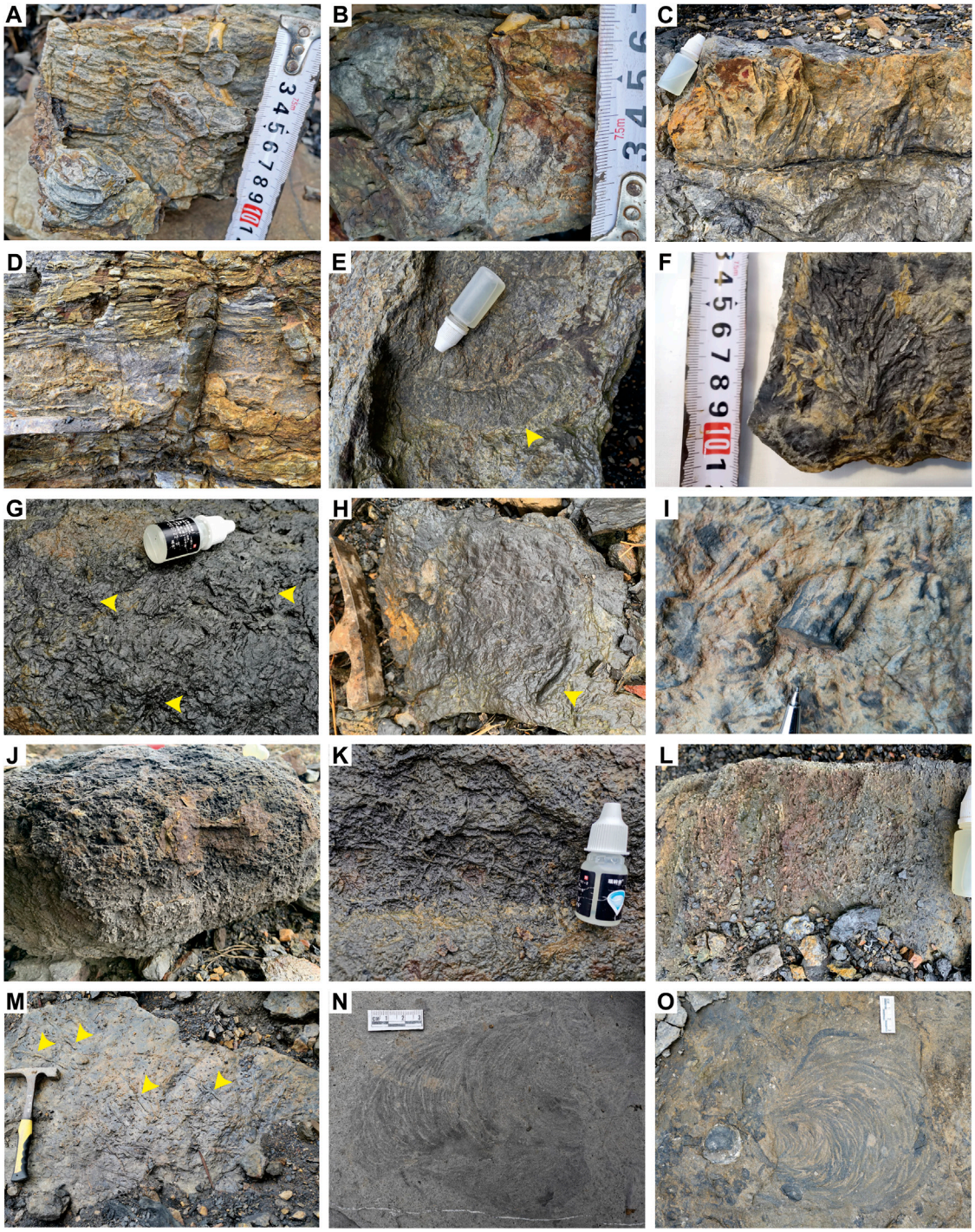

FIGURE 8
Trace fossils in the Jiusi Formation. **(A–C)** Cross-section view of the *Skolithos linearis* in lithofacies Sb (bioturbated sandstones). **(A,B)** Section LDZ; **(C)** section DHZ; cross-section view **(D)** and bedding-plane view **(E)** of the *Ophiomorpha* isp. In lithofacies Sb, section LDZ. **(F,G)** Bedding-plane view of the *Chondrites filifalx* in lithofacies Hb **(F)** and lithofacies Mb **(G)**, section LDZ **(H,I)** bedding-plane view, and **(H)** cross-section view of the *Palaeophycus* sp. In lithofacies Sb, section LDZ. **(J–L)** The bioturbated siltstone and trace fossils were dominated by *Chondrites* sp. **(J)** Cross-section view **(K)** and bedding-plane view **(L)** of **(J)**. **(M)** *Planolites* sp. In lithofacies Sb, section LDZ. **(N,O)** Bedding-plant view of *Zoophycos cf. shandongensis* **(N)** and *Zoophycos* sp. **(O)** section LDZ.

FIGURE 9
Facies association 3 in section YGX. **(A)** Finning upwards sequence in a submerged fluvial environment. **(B)** Lithofacies Mp (Phytophoric mudstone) with abundant lepidophyte leaves, in a submerged natural levee setting. **(C)** lepidophyte trunk, floodplain setting. **(D)** The boundary (yellow dashed line) of lithofacies Mp and lithofacies Ss (structureless sandstones), an erosional base together with sandstones structure suggest a submerged distributary channel deposit. **(E)** The sheet sandstone was penetrated by finger-like mudstones, in a distal delta front setting. **(F)** Lithofacies Ms (sigmoidal mudstones) with a dip direction towards the lagoonal environment (yellow dashed line), in a prodelta setting.

Planolites and *Palaeophycus* in lithofacies Mb and Hb, indicates a relatively organic-rich, oxygen-deficient tidal zone.

5.2.3 Facies association 3 (Lithofacies M, Mp, Ms, Ss, Sc): delta deposits

Facies association 3 occurs only in the lower part of the YGX section. Despite the fact that this section is not completely outcropped, the lithological sequence of a delta facies can be identified. It begins with phytophoric mudstones (lithofacies Mp) interbedded with structureless sandstones (lithofacies Ss), ascends to lithofacies Ss and mudstones (lithofacies M), ending up with sigmoidal mudstones (lithofacies Ms). These associations indicated a prograde cycle of delta during a transgression. Lithofacies Mp contains frequent plant fossils with well-preserved leaves and trunks, suggesting a delta plain setting (Figure 9C). The interbedded siltstone (dozens of centimeters thick) with fine upward cycles suggests an abandoned channel deposit. Passing upwards to lithofacies Ss with an erosional base and a finning upward granulometry suggests a submerged distributary channel deposit (Figure 9A). The plant fossil fragment on the top of the mud-siltstone indicates a submerged nature levee environment (Figure 9B). The well-sorted and thick structureless sandstones (lithofacies Ss) with an erosional base (Figure 9D) suggest a mouth bar or a distal bar setting. The upmost part of Facies association 3 consists of thin siltstones and of lithofacies Ms, the sheet siltstone is frequently penetrated by finger-like mudstones laterally (Figure 9E), indicating a typical distal delta front lithofacies (Wang and Zhang, 1996). The lithofacies Ms usually cap upon the sheet-like siltstones with interbedded sigmoidal deformation structures, and they are inclined seaward (Figure 9F). The interbedded sigmoidal deformation mechanism may be related to the source supply capacity; when the source supply was strong, the delta complex advanced seaward, particularly, a great part of the silt- and clay-size material of river load was deposited along the prodelta (Einsele, 1992), when the mudstones accumulate huge thickness along the prodelta slope, while soft sediments trend to collapse seaward under the force of gravity. Therefore, Facies association 3 was considered as a fluvial-dominated delta.

The trace fossils of the Facies association 3 are rare; only a few *Palaeophycus* were found within mudstone horizons. Given the wide distribution of *Palaeophycus*, which ranges from terrestrial to deepwater environments (Yang et al., 2004), there is no sedimentary significance to the identified facies.

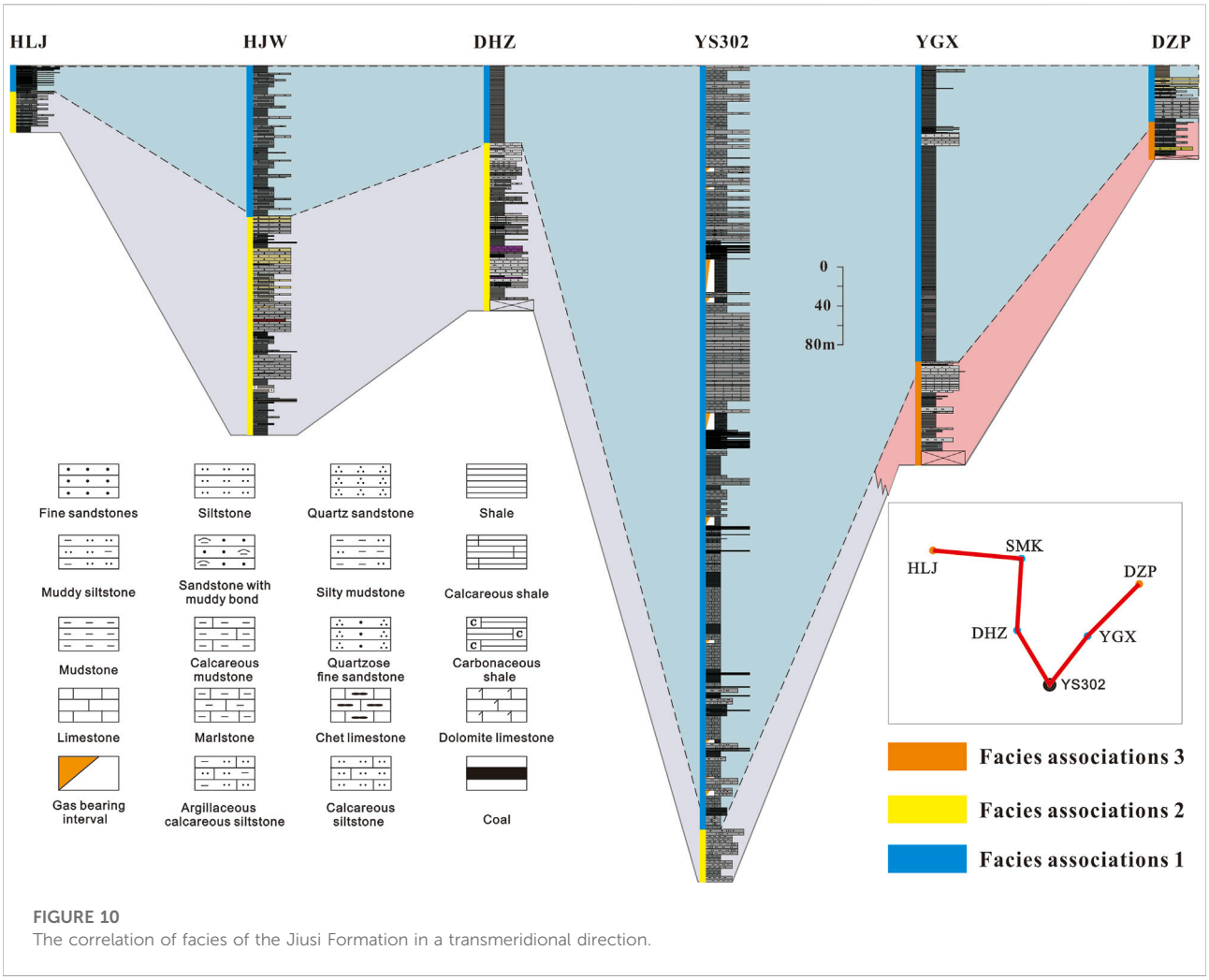

FIGURE 10
The correlation of facies of the Jiusi Formation in a transmeridional direction.

5.2.4 Vertical evolution of facies associations and sedimentary facies distribution of the Jiusi Formation

The sedimentary facies of the Lower Carboniferous Jiusi Formation in the Weining area can be divided into two parts. The lower part of the Jiusi Formation is represented mainly by a tidal facies (Figures 10, 11), the delta facies only occurred in the YGX section (Figure 10); the upper part of the Jiusi Formation includes lagoon deposits (Figures 10, 11). The evolution of sedimentary facies of the Jiusi Formation shows a process of continuous transgression under the background of tectonic syn-subsidence during the early Carboniferous around the Weining area. At the beginning of the deposition of the Jiusi Formation, tidal deposits dominated most of the Weining area, except for the YGX section, which was closer to the hinterland (Figure 4A), with fluvial-dominated delta deposits. Following the continuous extension of synsedimentary faults as well as following the transgression, it finally evolved into lagoonal facies deposition. The tidal deposits are mainly developed along with horst assemblages in synsedimentary faults, while the graben assemblages are dominated by lagoon deposits. The transformation rates of sedimentary facies are also different, related to step-fault combinations at the graben assemblage, to faster basement subsidence rates and to deeper water conditions. In this way, the tidal face associations were transformed into lagoon facies earlier. Taking the YS302 facies associations as an example, the thickness of lagoonal associations content reaches 93.5%, while the tidal face associations content only accounts for 6.5% of the Jiusi Formation. Although the synsedimentary extension-rift also caused thinning of the crust and subsidence of the whole basement along with increasing accommodation compared with the morphology of the graben assemblage, a relatively shallower water condition in the horst zone was less impacted by synsedimentary depression under enough sources of supply. The thickness of tidal face associations content in the horst zone (90.2%) is much greater than the lagoonal associations (9.8%), with repeated overlapping intertidal lithofacies associations at the LDZ section, further transformed into lagoonal settings.

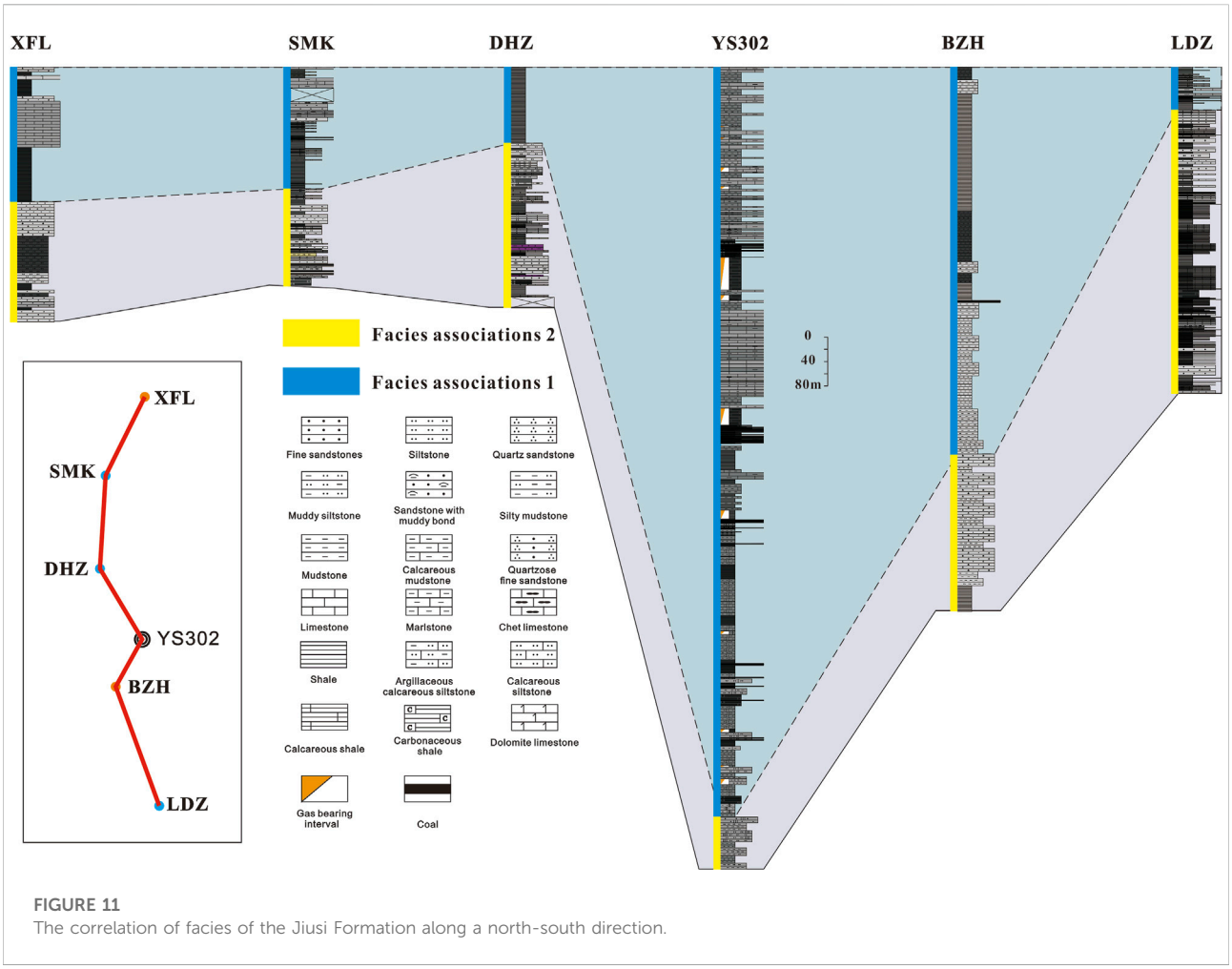

FIGURE 11
The correlation of facies of the Jiusi Formation along a north-south direction.

Based on these observations, a facies distribution of the Jiusi Formation is proposed (Figure 12). The stratigraphic thickness and facies associations of Jiusi Formation were controlled by the synsedimentary extension-rift activity of the northwestern Liupanshui Depression. In the northeast of the study area, supratidal subfacies are developed around the hinterland and a fluvial-dominated delta facies is set along the DZP to YGX section. As the activity of the step-fault zone intensified, the water in the synsedimentary elongated trough deepened gradually, and the lagoon-facies deposition controlled by the NW fault was formed from YS302 to the southeast of the study area. The other parts are mainly tidal facies.

5.3 Shale gas reservoir exploration potential of Jiusi Formation

Planning and designing a successful shale gas exploration block generally depends on the geological evaluation system of the shale quality (Guo, 2014; Jin et al., 2016). Based on some shale gas mining test areas and on the successful experience of other countries, combined with China's own geological characterstics, some parameters for evaluation standards of shale quality targets on optimization were proposed, including TOC content, thermal maturity, silica content, porosity, gas content, and rock mechanical parameters (Zeng et al., 2015; Ma et al., 2018; Jiang et al., 2019a). These standards have their own characterstics and a relative board research object involves Palaeozoic marine and lacustrine shales and Mesozoic-Cenozoic terrestrial shales. However, given the variable tectonics, sedimentary setting, and geomorphic and topographic conditions of the Jiusi shale, some parameters (such as TOC, Ro) of evaluating standards cannot effectively help evaluate the optimization of favorable Jiusi shale horizon. There is no favorable horizon for shale gas exploration of YS302, with strictly followed by the above standards, especially when compared with the marine shales that have been successfully exploited commercially. The quality of the Jiusi transitional shale is relatively poor.

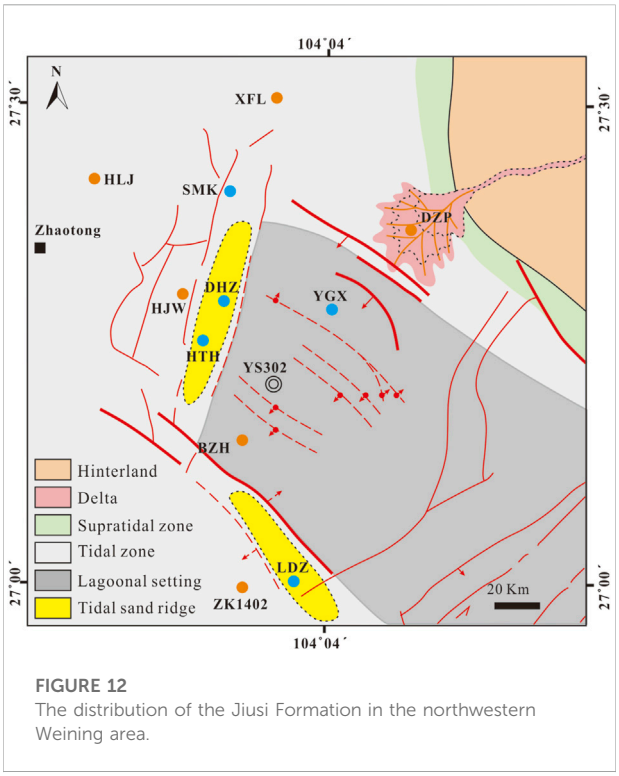

FIGURE 12
The distribution of the Jiusi Formation in the northwestern Weining area.

On the contrary, the Jiusi shale during the drilling of YS302 showed abnormal gas logging in dozens of horizons, and the water immersion test of the core section revealed continuous bubble release and upwelling with a size of between 0.5 and 1.5 mm and lasting for a long time (Figure 13). This result indicates the Jiusi transitional shale has great potential for shale gas exploration. For better evaluating the development of Jiusi transitional shale, we scaled down some key evaluation parameters and reenacted a shale reservoir evaluating standard based on the above marine shale reservoir standard and on the testing results of the Jiusi shale (Table 5).

Reenacted evaluated standard focuses on the shale reservoir parameters adjustment such as TOC content, porosity, shale horizon thickness, lithofacies, and gas content. Considering that the shale gas reservoir is a typical artificial reservoir, the production of shale gas relates to subsequent hydraulic fracturing efficiency, the content of brittle minerals in shale play an important role in the fracability, affecting the brittleness, fracture development, and fracture mode of shale (Zou et al., 2010; Ding et al., 2016; Zhang et al., 2017; Zhong et al., 2018). The brittle mineral content of most Jiusi transitional shale exceeds 40%, even exceeding 60% from 1,347.5 to 1991.6 m depths, indicating that the Jiusi shale is prone to the formation of fracture networks after fracturing.

According to the reenacted evaluated standard, two types of shale reservoirs were clarified in YS302 (Table 6), establishing that the favorable shale horizon accumulative thickness is 104m and that the lithofacies were dominated by carbonaceous shale interbedded with coal seams.

5.4 Comparison of the properties of the transition shale and of the marine shale

Compared with the marine shale of the Ordovician - Silurian Wufeng-Longmaxi Formations in the Jiaoshiba area (Table 7), the Jiusi transitional shale shows relatively poor quality. Some key values of the Jiusi Formation are different from those of marine shales, such as gas content, TOC content, and effective porosity. The reason may be related to the water depth during the shale deposition, as the oxygen content of the inner shelf of the Wufeng-Longmaxi Formation was extremely low, and no bioturbation was reported. The upper Jiusi shale in the lagoonal setting contains a large number of trace fossils, and the activity of organisms disrupted the conditions of preservation of organic matter. Moreover, lagoonal shale is more susceptible to climate and sea-level change. Under a warm and humid climate as well as during a sea-level drop, the increased terrestrial input may cause organic matter to dilute and decompose. Consequently, the TOC content of the Jiusi Formation showed a strong heterogeneity (Figure 14), while the TOC content of the Wufeng-Longmaxi marine shale increases with the water depth (Ma et al., 2018), as the marine shale of the inner shelf is relatively less affected by sea-level change. The content of water-sensitive minerals in the Jiusi shale is relatively high, with the average content of illite/smectite mixed-layer in clay minerals of 52.84%. The tendency of high content illite/smectite mixed-layer to swell macroscopically and its cause of shale instability in well drilling operations can potentially lead to collapse of the wellbore (Anderson et al., 2010). Meanwhile, the damage from expanding clays in cores can reduce the effective throat radius with scatting of the paragenetic structures of clay minerals, further influencing the shale gas production during hydraulic fracturing (Liao et al., 2012). Therefore, new technology and supporting equipment are needed for developing the Jiusi shale. Nevertheless, the lagoon facies is prone to forming thick coal seams during the process of sea-level fall (Zhu, 2008), and the preservation of *in-situ* coal seams is relatively high. This shows that shale gas and coalbed methane can be developed together.

6 Conclusion

(1) The thickness distribution of the Jiusi Formation in the Weining area was controlled by the sysedimentary extension faults of the northwestern Liupanshui Depression, with the depositional center of the Jiusi Formation extending in a NW direction and asymmetrically thinning in a NE–SW direction.

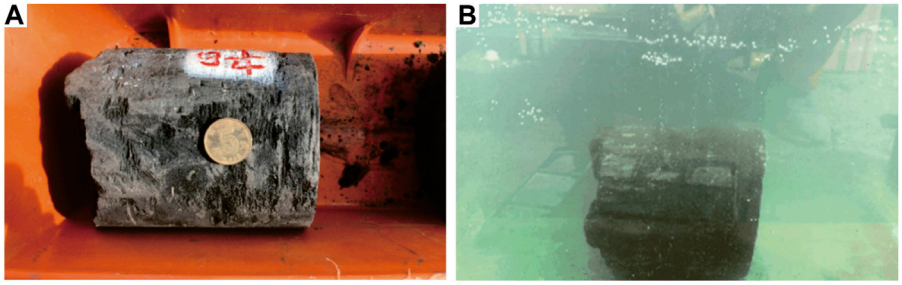

FIGURE 13
Water immersion testing of a core section in YS302 (1724.17–1724.28 m) (Mei et al., 2021).

TABLE 5 New evaluation standards for the YS302 shale reservoir.

Evaluation parameters	Type-II reservoir	Type-III reservoir
Gas content	≥2%	≥1%
TOC content	≥1%	≥1%
Effective porosity	≥2%	≥1%
Brittle mineral content	≥60%	≥60%
Thickness	≥10 m	≥10 m
Lithofacies	Lithofacies M	Lithofacies M

TABLE 6 Evaluation of the YS302 with new standards.

Depth (m)	Thickness (m)	Minerals (%)					Other parameters (%)			Reservoir types
		Quartz + feldspar	Carbonatite	Pyrite	Clay	Brittle mineral	TOC	Effective porosity	Gas content (m^3/t)	
1711.2–1724.5	13.3	34.8	48.8	1.5	13.8	83.6	1.0	2.5	1.9	II-III
1896.4–1909.8	13.4	19.4	56.6	0.6	22.1	76.0	1.1	1.9	1.8	III
1913.6–1939.3	25.7	22.1	50.5	0.6	25.6	72.6	1.0	1.8	1.8	III
1942.6–1968.5	25.9	32.1	37.8	1.0	27.9	69.9	1.1	1.7	1.7	III
1991.6–2004.1	12.5	16.0	49	0.8	32.9	65.0	1.3	3.2	3.1	II
2058.8–2081.4	22.6	20.2	42.8	0.6	35.2	63.0	1.1	1.7	1.6	III

TABLE 7 Comparison of key parameters of sweet pot shale reservoir between YS302 and the Jiaoshiba area. Shale reservoir dataset of the Jiaoshiba area summarized from (Ma et al., 2018).

Location	Stratum	Facies	Key parameters of shale reservoir (average)			
			TOC content	Gas content	Effective porosity	Brittle mineral content
YS302	Jiusi Fm.	lagoon	1.1%	~2 m^3/t	2.1%	71.7%
Jiaoshiba area	Wufeng-Longmaxi Fm.	Inner shelf	>3%	>6 m^3/t	>5%	~60.0%

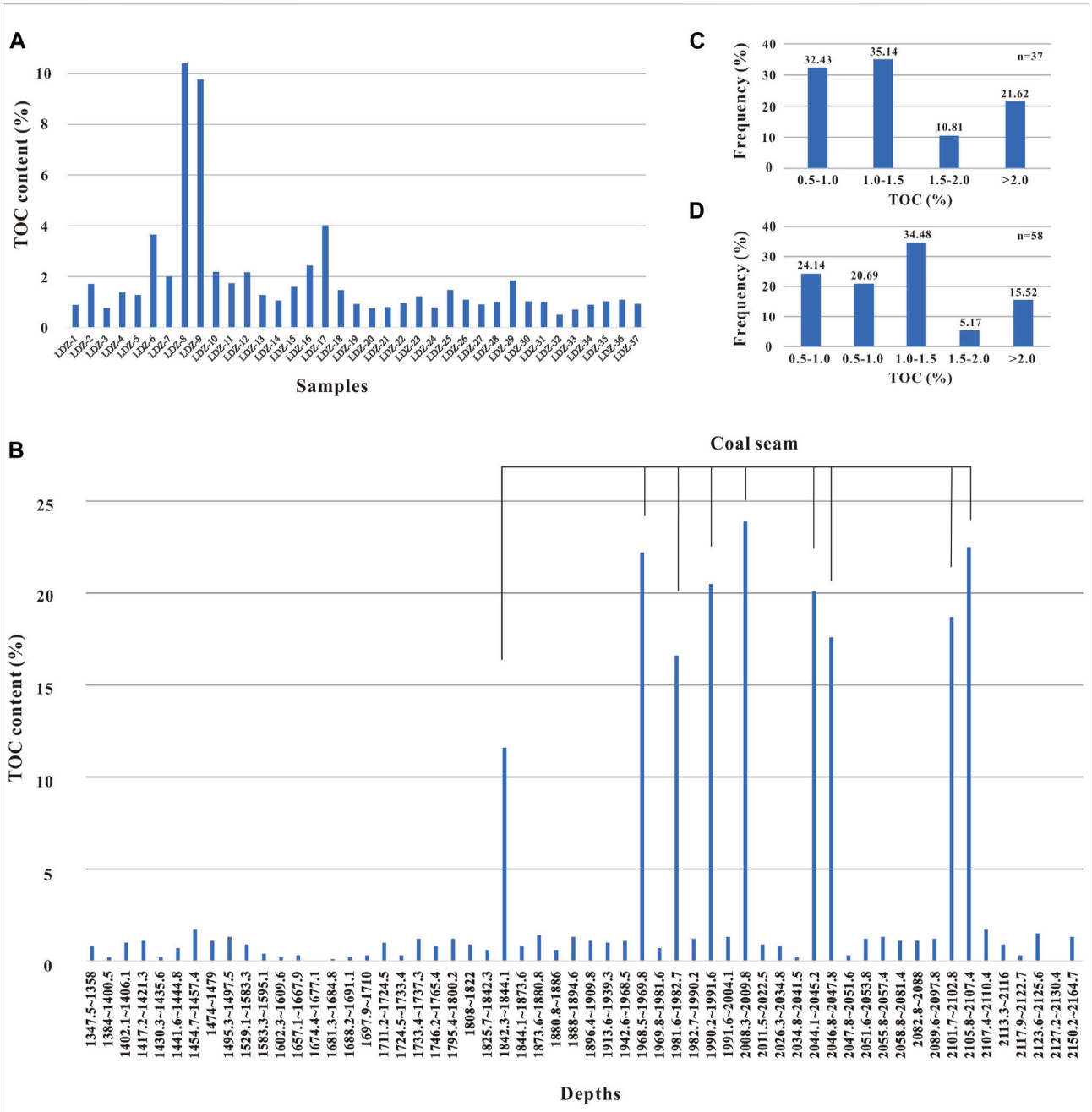

FIGURE 14
The TOC content of the Jiusi Formation. **(A)** TOC content from section LDZ, **(B)** TOC content from the logging interpretation of YS302, all horizons with TOC greater than 2% are coal seams. The TOC histogram of section LDZ **(C)** and YS302 **(D)**.

(2) The sedimentary facies of the Lower Carboniferous Jiusi Formation in the Weining area can be divided into two members. The lower member of the Jiusi Formation records mainly tidal facies, while the delta facies only occurred in the YGX section; the upper member of the Jiusi Formation was deposited under lagoonal conditions. The facies associations of the Jiusi Formation are also controlled by sysedimentary extension faults. The tidal deposits are mainly developed along horst assemblages, while the graben assemblages are dominated by lagoon deposits.

(3) Compared with the marine shale of the Ordovician - Silurian Wufeng-Longmaxi Formations in north Guizhou and Yunnan provinces, the Jiusi transitional shale shows relatively poor quality for some key parameters. The evaluation standard for marine shale cannot be applied to the transitional Jiusi shale. After appropriate reductions in some evaluation proxies, there is

still nearly 100 m of cumulative thickness shale in YS302 worthy of shale gas development. Considering that transitional shales are often interlayered with coal seams, the shale gas and the coalbed methane can be developed together.

Data availability statement

The original contributions presented in the study are included in the article/supplementary material; further inquiries can be directed to the corresponding author.

Author contributions

JZ wrote the manuscript, TZ, WY, and HZ reviewed and modified the manuscript, ZZ provided the dataset of YS302, HL, YB, and LG helped with fieldwork in Weining.

Funding

This study was co-sponsored by the Science and Technology Cooperation Project of the CNPC-SWPU innovation alliance no. 2020CX050103, and by the National Natural Sciences Foundation of China (Nos. 41972120, and 42172129).

Acknowledgments

We sincerely thank the Zhejiang Oilfield Company for the technical and fieldwork support. We thank Professor Hu Bin, Henan Polytechnic University, for help with identifying trace fossils, we also thank Professor Mihai Emilian Popa, University of Bucharest, for improving our manuscript.

Conflict of interest

ZZ was employed by Zhejiang Oilfield Company.

The remaining authors declare that the research was conducted in the absence of any commercial or financial relationships that could be construed as a potential conflict of interest.

Publisher's note

References

Alvarez, W., Engelder, T., and Lowrie, W. (1976). Formation of spaced cleavage and folds in brittle limestone by dissolution. *Geol.* 4, 698. doi:10.1130/0091-7613(1976)4<698:foscaf>2.0.co;2

Anderson, R. L., Ratcliffe, I., Greenwell, H. C., Williams, P. A., Cliffe, S., Coveney, P. V., et al. (2010). Clay swelling – a Challenge in the oilfield. *Earth-Science Rev.* 98 (3-4), 201–216. doi:10.1016/j.earscirev.2009.11.003

BGMEDGP (Bureau of Geology and Mineral Exploration and Development Guizhou Province) (1973). *Regional geology of Guizhou province*. Beijing: Geological Publishing House.

BGMEDGP (Bureau of Geology and Mineral Exploration and Development Guizhou Province) (1987). *Regional geology of Guizhou province*. Beijing: Geological Publishing House.

BGMEDGP (Bureau of Geology and Mineral Exploration and Development Guizhou Province) (2017). *Regional geology of Guizhou province*. Beijing: Geological Publishing House.

Bromley, R. G., and Ekdale, A. A. (1984). Chondrites: A trace fossil indicator of anoxia in sediments. *Science* 224, 872–874. doi:10.1126/science.224.4651.872

Cao, Qichen, Huang, Bo, Yang, Tao, Zhang, Yinfeng, Guo, Baichuang, Fan, Zhongxue, et al. 2019. Further discussion on the geotectonic characteristics of Guizhou province, China. Nonferrous Metals (Mining section), 71(06):59–65. doi:10.3969/j.issn.1671-4172.2019.06.012

Chen, Guofan, and Xu, Anquan (1998). An insight into the northwestern-trending tectonical deformation of the Weining-Ziyun belt, Western Guizhou. *Geol. Guizhou* 15 (04), 311–320.

Chen, Rong, and Zhang, Ziya (2020). *Sedimentary environment and palaeogeographical pattern of the early carboniferous late yanguan- early datang stage in eastern yunnan-western Guizhou*. China: Geological Bulletin of China. Online published.

Ding, Wenjiang (1931). Stratification of fengning series. *Acta Geol. Sin.* 10, 31–48.

Ding, Wenlong, Zeng, Weite, Wang, Ruyue, Kai, Jiu, Wang, Zhe, Sun, Yaxiong, et al. (2016). Method and application of tectonic stress field simulation and fracture distribution prediction in shale reservoir. *Earth Sci. Front.* 23 (2), 63–74. doi:10.13745/j.esf.2016.02.008

Einsele, Gerhard (1992). "Depositional systems and facies models," in *Sedimentary basins: Evolution, facies, and sediment budget* (Verlag Berlin: Springer), 18–272.

GCGB (Guizhou Coalfield Geological Bureau) (2013). *Investigation and evaluation of shale gas resource in Southwest Guizhou*. Guiyang: Guizhou Coal Mine Geological Engineering Consulting and Geological Environment Monitoring Center.

Guo, Xusheng (2014). Rules of two-factor enrichment for marine shale gas in southern China: Understanding from the Longmaxi Formation shale gas in Sichuan Basin and its surrounding area. *Acta Geol. Sin.* 88 (07), 1209–1218.

Hein, J. R., and Karl, S. M. (1983). "Comparisons between open-ocean and continental margin chert sequences," in *Siliceous deposits in the pacific region. Developments in sedimentology*. Editors A. Lijima, J. R. Hein, and R. Siever (Amsterdam: Elsevier), 36, 25–43.

Jiang, Yuqiang, Fu, Yonghong, Xie, Jun, Dong, Dazhong, Zhou, Keming, Cheng, Xiaoyan, et al. (2019a). Development trend of marine shale gas reservoir evaluation and a suitable comprehensive evaluation system. *Nat. Gas. Ind.* 39 (10), 1–9. doi:10.3787/j.issn.1000-0976.2019.10.001

Jiang, Yuqiang, Liu, Xiongwei, Fu, Yonghong, Hu, Chen, Zhang, Haijie, Yan, Jun, et al. (2019b). Evaluating of effective porosity in marine shale reservoir, Western Chongqing. *Acta Pet. Sin.* 40 (10), 1233–1243. doi:10.7623/syxb201910008

Jin, Zhijun, Hu, Zongquan, Gao, Bo, and Zhao, Jianhua (2016). Controlling factors on the enrichment and high productivity of shale gas in Wufeng-Longmaxi Formations, Southeastern Sichuan Basin. *Earth Sci. Front.* 23 (01), 1–10. doi:10.13745/j.esf.2016.01.001

Le, Guangyu (1991). A new discussion on the tectonic framework in Liuzhi-Panxian-Shuicheng region, Guizhou. *Geol. Guizhou* 8 (04), 289–301.

Li, Kai (2016). Shale gas accumulation condition of lower carboniferous Jiusi Formation in weining – shuicheng. *Special Oil Gas Reservoirs* 23 (05), 48–61. doi:10.3969/j.issn.1006-6535.2016.05.011

Liao, Jijia, Tang, Hongming, Zhu, Xiaomin, Ren, Mingyue, Sun, Zhen, and Lin, Dan (2012). Water sensitivity experiment and damage mechanism of sandstone reservoirs with ultra-low permeability: A case study of the eighth oil layer in yanchang formation of xifeng oilfield, ordos basin. *Oil Gas Geol.* 33 (02), 321–327. doi:10.11743/ogg20120220

Lu, Shufan, Yi, Chen, Luo, Xiangjian, He, Ben, and Fu, Hongbin (2021). Sedimentary characteristics and distribution of the carboniferous black shale in Guizhou province. *Acta Sedimentol. Sin.* 39 (03), 672–685. doi:10.14027/j.issn.1000-0550.2020.114

Ma, Yongsheng, Cai, Xunyu, and Zhao, Peirong (2018). China's shale gas exploration and development: Understanding and practice. *Petroleum Explor. Dev.* 45 (4), 589–603. doi:10.1016/s1876-3804(18)30065-x

MacEachern, J. A., Bann, K. L., Gingras, M. K., Zonneveld, J.-P., Dashtgard, S. E., and Pemberton, S. G. (2012). "The ichnofacies paradigm," in *Trace fossils as indicators of sedimentary environments. Developments in sedimentology*. Editors D. Knaust and R. G. Bromley (Amsterdam: Elsevier), 64, 103–138.

Mao, Jianquan (1997). The Geological characteristics and tectonic evolution of Shuicheng fault subsidence. *Fournal Guizhou Univ. techmology* 26 (02), 1–9.

Mei, Jue, Ji, Yubing, Ren, Jinglun, Zhang, Hanbing, and Zhou, Yun (2021). Shale gas accumulation conditions in the lower carboniferous Jiusi Formation of dianqianbei depression. *Nat. Gas. Ind.* 41 (S1), 51–59. doi:10.3787/j.issn.1000-0976.2021.S1.007

MNRC (Ministry of Natural Resources of China) (2018). *China mineral resources (2018)*. Beijing: Geological Publishing House.

Murchey, B. L., and Jones, D. L. (1992). A mid-permian chert event: Widespread deposition of biogenic siliceous sediments in coastal, island arc and oceanic basins. *Palaeogeogr. Palaeoclimatol. Palaeoecol.* 96, 161–174. doi:10.1016/0031-0182(92)90066-e

Qin, Qin, Long, Chengxiong, and Tang, Xiangui (2016). Analysis of carboniferous Jiusi Formation shale sedimentary environment in southwestern Guizhou. *Goal Geol. China* 28 (4), 35–40. doi:10.3969/j.issn.1674-1803.2016.04.07

Shi, Mingke, Huang, Bo, Yao, Yang, Xu, Weijun, Li, Daji, Peng, Li, et al. (2019). A brief analysis of geotectonics and distribution of mineral deposits of Guizhou province. *Acta Geol. Sichuan* 39 (04), 536–541. doi:10.3969/j.issn.1006-0995.2019.04.002

Sun, Qisen (2016). *Study on sequence stratigraphy and evolution of paleogeography for Carboniferous – zisongian stage Permian in northeast of Yunnan and adjacent area*. Kunming: Kunming University of Science and Technology.

Tang, Xiangui, Liu, Taiqin, Xiao, Hong, Xu, Wenhui, and Liu, Feng (2016). Prospects of shale gas in lower carboniferous Jiusi Formation, weining area. *Nat. Gas Technol. Econ.* 10 (5), 23–27. doi:10.3969/j.issn.2095-1132.2016.05.006

Tang, Xiangui, Qin, Wen, Qin, Qin, Gao, Wei, and Luo, Sha (2014). Upper paleozoic group shale gas resources analysis in southwestern Guizhou province. *Coal Geol. China* 26 (06), 1–4. doi:10.3969/j.issn.1674-1803.2014.06.01

Taylor, A. M., and Goldring, R. (1993). *Description and analysis of bioturbation and ichnofabric*, 150. London: Geological Society of London, 141–148.

Wang, Liangchen, and Zhang, Jingliang (1996). *Sedimentary environment and sedimentary facies*. Beijing: Petroleum Industry Press.

Wang, Pengwan, He, Yong, Li, Junjun, Huang, Ling, Jiang, Liwei, Li, Xianjing, et al. (2020). Paleoenvironmental characteristics of the Jiusi Formation and potential for shale gas exploration in Zhaotong shale gas demonstration zone. *J. China Coal Soc.* 45 (10), 3840–3491. doi:10.13225/j.cnki.jccs.2019.0996

Wang, Shangyan, Zhang, Hui, Wang, Tianhua, Wang, Chunhou, Peng, Chenglong, Hu, Renfa, et al. (2006). Filling and evolution of the late paleozoic shuicheng-ziyun aulacogen in Western Guizhou, China. *Geol. Bull. China* 25 (03), 402–407. doi:10.3969/j.issn.1671-2552.2006.03.010

Wang, Xinwei, Guo, Tonglou, Yujin, Wo, Zhou, Yan, Wu, Lizhi, Zhang, Rongqiang, et al. (2013). Characteristics of deep structural segmentation and transformation of the Yaziluo fault zone. *Oil Gas Geol.* 34 (02), 220–228. doi:10.11743/ogg20130213

Xia, Bangdong, and Liu, Honglei (1992). The Yunnan-Guizhou- Guangxi rift system. *Exp. Pet. Geol.* 14 (01), 20–30.

Yang, Gang (2020). *Sedimentary characteristics and basic geological conditions of shale gas in lower carboniferous Jiusi Formation in weining area, southwest Guizhou*. Chengdu: Chengdu University of Technology.

Yang, Shipu, Zhang, Jianping, and Yang, Meifang (2004). *Trace fossils of China*. Beijing: Science Press.

Zeng, Qiunan, Zhou, Guixin, Yu, Bingsong, Ziqi, Feng, and Miao, Miao (2015). Evaluation criteria of lake facies shale gas reservoir: A case study of the organic rich shale developed in yanchang group, ordos basin. *Xinjiang Geol.* 33 (03), 409–414. doi:10.3969/j.issn.1000-8845.2015.03.026

Zeng, Yunfu, Liu, Wenjun, Chen, Hongde, Zheng, Rongcai, and Zhang, Jinquan (1995). Evolution of sedimentation and tectonics of the Youjiang composite basin, South China. *Acta Geol. Sin.* 69 (2), 113–124.

Zhang, Chenchen, Dong, Dazhong, Wang, Yuman, Jiang, Shan, and Guan, Quanzhong (2017). Research progress on brittleness of shale reservoirs. *Xinjiang Pet. Geol.* 38 (01), 111–118. doi:10.7657/XJPG20170120

Zhang, Jing (2015). *Study on trace fossils and paleoenvironment of Changhsingian (Late Permian) in northeastern Sichuan basin*. Chengdu: Southwest Petroleum University.

Zhang, Zhengshan (2017). *Sedimentary environment evolution of lower carboniferous Jiusi Formation in weining area*. Chengdu: Southwest Petroleum University.

Zhong, Cheng, Qin, Qirong, Zhou, Jiling, Hu, Dongfeng, and Wei, Zhihong (2018). Brittleness evaluation of organic-rich shale in Longmaxi Formation in Dingshan area, southeastern Sichuan. *Geol. Sci. Technol. Inf.* 37 (04), 167–174. doi:10.19509/j.cnki.dzkq.2018.0422

Zhu, Xiaomin (2008). *Sedimentary petrology*. 4th edition. Beijing: Petroleum industry press.

Zou, Caineng, Dong, Dazhong, Wang, Shejiao, Li, Jiangzhong, Li, Xinjing, Wang, Yuman, et al. (2010). Geological characteristics and resource potential of shale gas in China. *Petroleum Explor. Dev.* 37 (06), 641–653. doi:10.1016/s1876-3804(11)60001-3

Zou, Caineng, Zhao, Qun, Dong, Dazhong, Yang, Zhi, Qiu, Zhen, Liang, Feng, et al. (2017). Geological characteristics, main challenge, and future prospect of shale gas. *Nat. Gas. Geosci.* 28 (12), 1781–1796. doi:10.1016/j.jnggs.2017.11.002